Understanding the Origin of the Regioselectivity in Non-polar [3+2] Cycloaddition Reactions through the Molecular Electron Density Theory

Luis R. Domingo,[1*] Mar Ríos Gutiérrez,[1,2] Jorge Castellanos Soriano[3]

[1] Department of Organic Chemistry, University of Valencia, Dr. Moliner 50, Burjassot, E-46100 Valencia, Spain.

[2] Department of Chemistry and Chemical Biology, McMaster University, 1280 Main Street West, Hamilton, Ontario L8S 4L8, Canada.

[3] Department of Chemistry, Polytechnic University of Valencia, Camí de Vera, s/n, 46022 Valencia, Spain.

E-mail: domingo@utopia.uv.es

Abstract

The regioselectivity in non-polar [3+2] cycloaddition (32CA) reactions has been studied within the Molecular Electron Density Theory (MEDT) at the B3LYP/6-311G(d,p) level. To this end, the 32CA reactions of nine simplest three-atom-components (TACs) with 2-methylpropane were selected. The electronic structure of the reagents has been characterised through the Electron Localisation Function (ELF) and the Conceptual DFT. The energy profiles of the two regioisomeric reaction paths and ELF of the transition state structures are studied to understand the origin of the regioselectivity in these 32CA reactions. This MEDT study permits to conclude that the least electronegative ends X1 atom of these TACs controls the asynchronicity in the C−X (X = C,N,O) single bond formation, and consequently, the regioselectivity. This behaviour is a consequence of the fact that the creation of the non-bonding electron density required for the formation of the new C−X single bonds has a lesser energetic cost at the least electronegative X1 atom than that at the Z3 one.

Keyword: non-polar [3+2] cycloaddition reactions; regioselectivity; molecular electron density theory; electronegativity.

1. Introduction

Cycloaddition reactions are one of the most useful tools to obtain cyclic compounds, due to their feasibility to create regio- and/or stereoselectively cyclic organic molecules [1,2]. [3+2] cycloaddition (32CA) reactions are an important class of cycloaddition allowing the formation of five-membered heterocycles of great pharmaceutical and industrial interest [3,4]. This kind of cycloaddition implicates the 1,3-addition of an ethylene derivative to a three-atom-component (TAC) (see Scheme 1). Depending on its structure, TACs can be classified as bent TACs (B-TACs) or linear TACs (L-TACs).
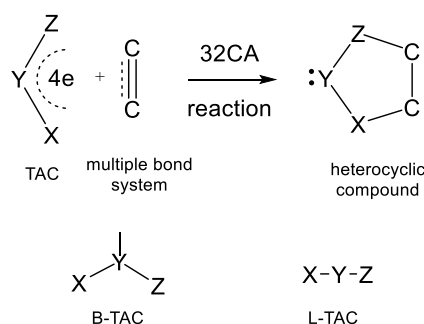
Scheme 1. 32CA reaction scheme and simplified Lewis structure of bent (B) and linear (L) TACs.

Many of the TACs participating in 32CA reactions are non-symmetric with respect to the central atom. When ethylenes, such as 1-substituted or 1,1-disubtituted ethylenes, are also non-symmetric, at least a pair of regioisomeric cycloadducts can be formed along the reaction (see Scheme 2). Unlike Diels-Alder (DA) reactions, which are highly regioselective yielding a unique cycloadduct [5], 32CA reactions are not as selective, yielding a mixture of the two feasible regioisomers. As regioisomers are structural isomers with physical and chemical different proprieties, only one of them will have a synthetic interest; consequently, formation of a mixture of two regioisomers involved a loss of the synthetic yield. Thus, the understanding of the origin of the regioselectivity in 32CA reactions is an important goal in order to predicts the formation of reaction mixtures.
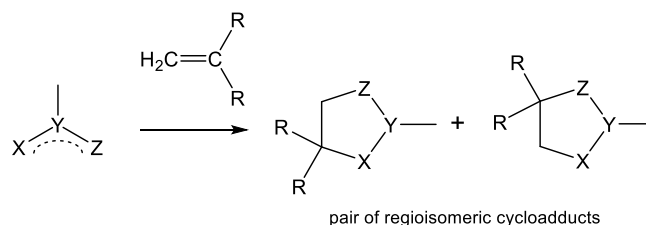

Scheme 2. Formation of regioisomeric cycloadducts in 32CA reactions involving non-symmetric reagents.

The regioselectivity of polar 32CA reactions was investigated in 2004 [6] by using the global and local reactivity indices defined within the Conceptual DFT (CDFT) [7,8]. That study suggested that for asynchronous 32CA reactions associated to polar processes, the regioselectivity is consistently explained by the most favourable two-center interactions between the highest nucleophilic and electrophilic sites of the reagents [6]. While the analysis of the electrophilicity [9] ω and nucleophilicity [10] *N* indices allows characterise the chemical proprieties of the reagents participation in polar processes, analysis of the Parr function [11] allows to characterise the most electrophilic and nucleophilic centers of a molecule. However, unlike DA reactions, many 32CA reactions have low even non-polar character, and consequently, the polar model to predict regioselectivity fail in this type of cycloaddition reactions.

In 2016 Domingo proposed the Molecular Electron Density Theory [12] (MEDT) for the study of the reactivity in Organic Chemistry, in which changes in the electron density, and not MO interactions, as the Frontier Molecular Orbital (FMO) theory proposed [13], are responsible for the feasibility of an organic reaction. In MEDT, several quantum-chemical tools based on the analysis of the electron density, such as the analysis of the CDFT reactivity indices [7,8], the topological analysis of the Electron Localisation Function (ELF) [14] and the Quantum Theory of Atoms in Molecules (QTAIM) [15] are used to rigorously study the chemical reactivity in Organic Chemistry [11].

Recent advances made in the theoretical understanding of 32CA reactions based on MEDT have allowed establishing a very good correlation between the electronic structure of simplest TACs and their reactivity towards ethylene [16]. Accordingly, depending on the electronic structure of the simplest TACs, *pseudodiradical*, *pseudoradical*, carbenoid and zwitterionic, 32CA reactions have been classified into *pseudodiradical* type *(pdr-type)*, *pseudomonoradical* type *(pmr-type)*, carbenoid type *(cb-type)* and zwitterionic type *(zw-type)* reactions [16], respectively, in such a manner that while *pdr-type* 32CA reactions can be carried out very easily, *zw-type* 32CA reactions demand adequate nucleophilic/electrophilic activations to take place (see Scheme 3).
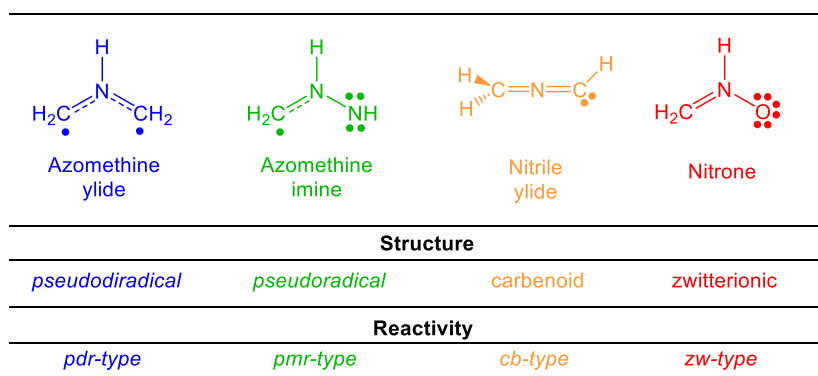
**Scheme 3.** Reactivity models associated to four different TAC structures.

On the order hand, organic reactions can also be classified as non-polar and polar reactions, in that way that organic reactions are favoured with the increase of the polar character of the reaction [17]. In 2014, Domingo proposed the analysis of the global electron density transfer (GEDT) [18,19] at the transition state structures (TSs) as a measure of the polar character of a reaction. Reactions with GEDT values below 0.05 e correspond to non-polar processes, while values above 0.20 e correspond to polar processes. Very recently, the organic reactions have been classified as the forward electron density flux (FEDF) and reverse electron density flux (REDF), depending on the direction of the flux of the electron density at the TS [20]. Non-polar reactions are classified as the null electron density flux (NEDF). This classification is unequivocal as the GEDT is a measure of the actual electron density transfer at the TSs. Thus, while the DA reaction between butadiene and ethylene was classified as the "normal electron demand"[21] within the Sustmann `s classification [22], it is classified as reaction of NEDF to be non-polar; note that the GEDT at this DA reaction is negligible, 0.0 e [23].

Many TACs as zwitterionic nitrones have nucleophilic character. Consequently, they react with electrophilic ethylenes such as methyl acrylate or nitroethylene through a polar mechanism with high regioselectivity [24]. In these polar *zw-type* 32CA reactions the analysis of the Parr function allows explaining the observed regioselectivity. However, TACs as nitrile oxides, which participate in *zw-type* 32CA reactions with low polar character, show low reactivity and low regioselectivity [25]. In addition, many ethylenes derivatives such as 2-methylpropane or styrene have not electrophilic character, and consequently, the corresponding 32CA reactions will have non-polar character. Note that many of the TACs have not electrophilic character as a consequence of the high electron density accumulation at the three centres of the TAC.

Since non-polar 32CA reactions have not been studied as much as polar 32CA reactions, the 32CA cycloadditions of the nine simplest TACs **1** to **9** shown in Table 1 with 2-methylpropane **10** are herein studied within MEDT in order to understand the origin of the regioselectivity in non-polar 32CA reactions (see Scheme 4).

Table 1. The atom composition, and name and the structural classification of the nine TACs **1** - **9** herein studied.

	X1-N2-Z3	Name	Structure
1	$H_2C{-}NH{-}CH_2$	azomethine ylide	bent
2	$H_2C{-}N{=}CH$	nitrile ylide	linear
3	$H_2C{-}NH{-}NH$	azomethine imine	bent
4	$H_2C{-}N{\equiv}N$	diazomethane	linear
5	$HC{=}N{=}NH$	nitrile imine	linear
6	$H_2C{=}NH{-}O$	nitrone	bent
7	$HC{-}N{\equiv}O$	nitrile oxide	linear
8	$NH{-}N{\equiv}N$	azide	linear
9	$N{=}N{-}O$	nitrous oxide	linear
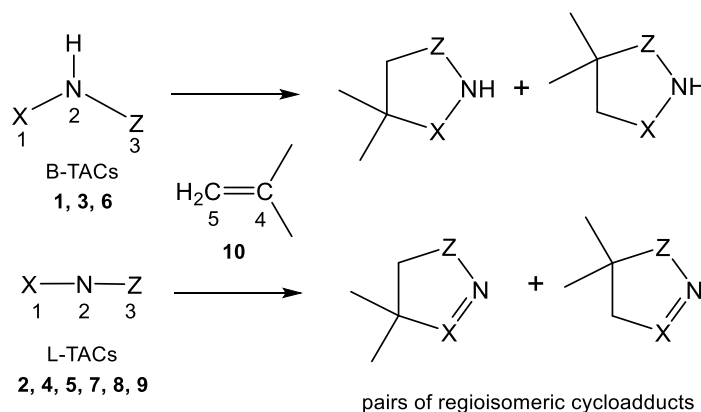
Scheme 4. Selected 32CA reactions of three bent, **1, 3** and **6**, and six linear, **2, 4, 5, 7, 8** and **9**, TACs with 2-methylpropene **10**.

2. Computational Methods

All stationary points were optimised using the B3LYP functional [26,27], together with the 6-311G(d,p) basis set [28]. The optimisations were carried out using the Berny analytical gradient optimisation method [29,30]. The stationary points were characterised by frequency computations in order to verify that TSs have one and only one imaginary frequency. The intrinsic reaction coordinate (IRC) paths [31] were traced in gas phase in order to check and obtain the energy profiles connecting each TS to the two associated

minima of the proposed mechanism, i.e. reactants and products, using the second order González-Schlegel integration method [32,33].

The electronic structures of the stationary points were characterised by NPA [34,35], and by the topological analysis of the ELF [14]. CDFT reactivity indices [7,8] were computed at the B3LYP/6-31G(d) level using the equations given in reference 8. The GEDT [18] was computed by the sum of the atomic charges (q) of the atoms belonging to each framework at the TSs; $GEDT = \Sigma q_f$.

All computations were carried out with the Gaussian 16 suite of programs [36]. ELF studies were performed with the TopMod program [37], using the corresponding B3LYP/6-311G(d,p) monodeterminantal wavefunctions and considering the standard cubical grid of step size of 0.1 Bohr. The molecular geometries and ELF basin attractor positions were visualised using the GaussView program [38], while the ELF localisation domains were represented by means of the Paraview software at an isovalue of 0.75 a.u. [39,40].

3. Results and Discussions

The present MEDT study has been divided into four parts: i) in section 3.1, a study of the electronic structure of TACs through an ELF topological and NPA analyses is performed; ii) in section 3.2, an analysis of the CDFT reactivity indices at the ground state (GS) of the reagents is carried out; iii) in section 3.3, a study of the reactivity and regioselectivity in the 32CA reactions of the nine TACs **1** - **9** with 2-methylpropene **10** is made; and finally iv) in section 3.4, an ELF topological analysis of the more favourable regioisomeric TSs is carried out in order to understand the changes in electronic density with respect to reagents, and thus, understand the origin of regioselectivity.

3.1. ELF Topological Analysis of reagents *1* to *10*

A useful correlation between the electronic structure and the reactivity of simplest TACs participating in 32CA reactions has been established [16]. ELF, first constructed by Becke and Edgecombe [14] and further illustrated by Silvi and Savin [41], permits stabilising a straightforward quantitative connection between the electron density distribution and the chemical structure. Consequently, the topological analysis of the ELF of the nine TACs **1** – **9** was performed to predict its reactivity in 32CA reactions [16]. In addition, the ELF of 2-methylpropene **10** was also analysed. The populations of the most significant valence

basins are listed in in Table 2, while the ELF basin attractor positions are given in Figure 1. A picture of the ELF localisation domains of four representative TACs characterising the four types of TACs, *pseudodiradical*, *pseudo(mono)radical*, carbenoid, zwitterionic, is shown in Figure 2. The ELF-based Lewis-like structures together with the natural atomic charges of the nine TACs are shown in Figure 1.

Table 2. Populations of the most significant ELF valence basin, in e, of the nine TACs **1 – 9** and 2-methylpropene **10**.

Basin	1	2	3	4	5	6	7	8	9	10
V(X1)	0.43	0.29	0.35	0.49	1.64			3.44	4.06	
V'(X1)	0.43	0.24	0.35	0.49						
V(X1,N2)	2.59	2.98	2.96	3.04	2.21	3.72	5.50	2.41	4.18	
V'(X1,N2)					2.27					
V(N2,Z3)	2.59	2.04	1.89	3.65	2.27	1.47	1.97	1.66	1.91	
V'(N2,Z3)		1.98						2.48		
V(Z3)	0.43	1.90	3.50	1.92	3.29	3.00	5.57	3.81	5.50	
V'(Z3)	0.43			1.92		2.84				
V(C4,C5)										1.76
V'(C4,C5)										1.76

At azomethine ylide **1**, two pairs of monosynaptic basins, V(C1) and V'(C1), and V(C3) and V'(C3), integrating a total of 0.86 e each pair, are observed at the C1 and C3 ends carbons. These ELF V(Ci) monosynaptic basins are related with the presence of two *pseudoradical* centers [42] at azomethine ylide **1**, thus being considered as a *pseudodiradical* TAC. Note that *pseudoradical* centers in a tetrahedric carbon are characterised by the presence of one V(C1) monosynaptic basin, while those in a trigonal planar carbon are characterised by the presence of two V(C1) and V'(C1) monosynaptic basins.

At azomethine imine **3** and diazoalcane **4**, two pairs of monosynaptic basins, V(C1) and V'(C1), integrating a total of 0.60 e and 0.98 e, respectively, are observed at the trigonal planar C1 carbon. For these TACs, these ELF V(C1) monosynaptic basins are related with the presence of one *pseudoradical* center at the C1 carbon of these TACs, thus being considered as a *pseudoradical* TACs.

At nitrile ylide **2** and nitrile imine **5**, one single V(Ci) monosynaptic basins, integrating 1.90 e (**2**) and 1.64 e (**5**), are observed at the C3 and C1 carbon, respectively, being associated to one carbenoid center, thus being considered **2** and **5** as carbenoid TACs. Note that nitrile ylide **2** also present two monosynaptic basins, V(C1) and V'(C1),

a total low population of 0.53 e, at the C1 carbon. (see Table 2) The V(Z3) monosynaptic basins present at these zwitterionic TACs, which are associated to N or O non-bonding electron density regions, correspond with the lone pair of the Lewis structures (see Figure 1).
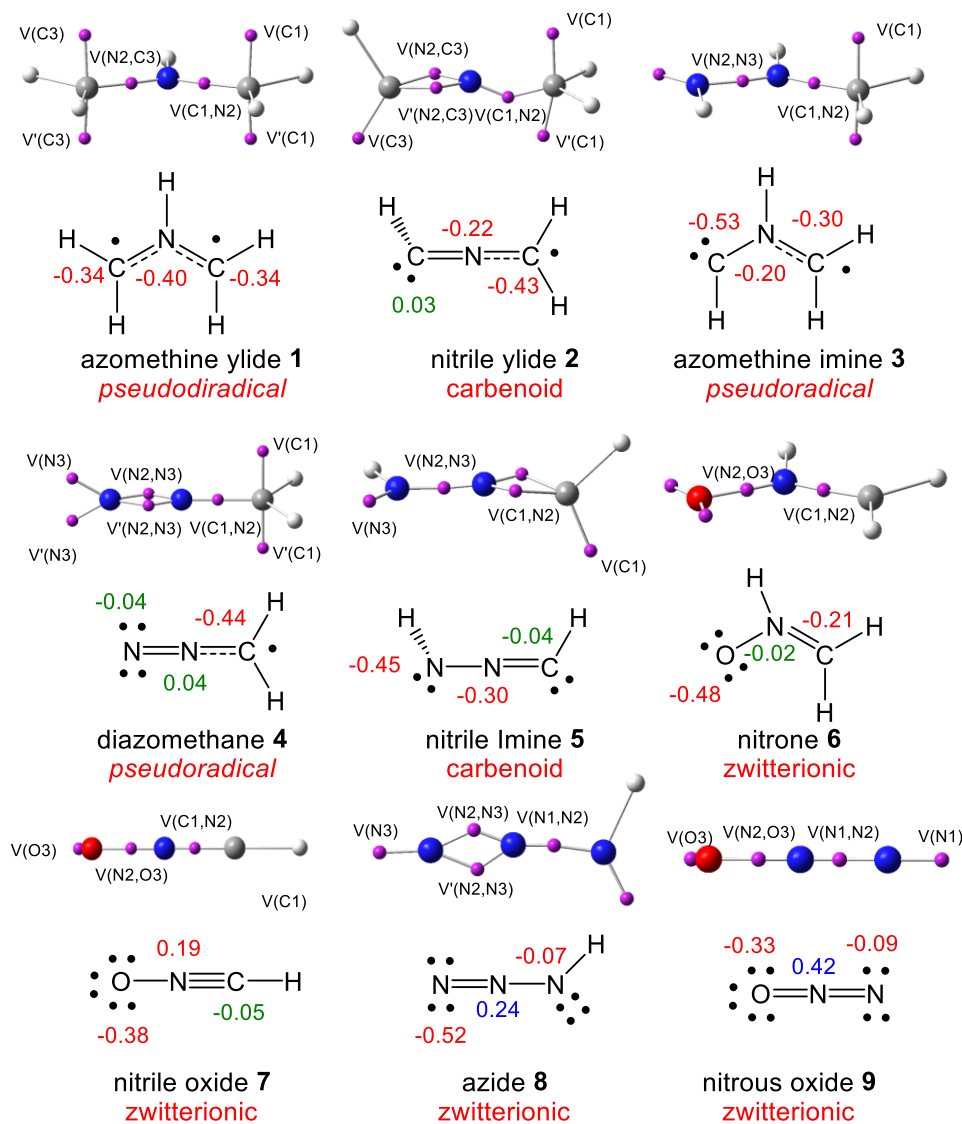

Figure 1. ELF basin attractor positions, ELF-based Lewis-like structures and TAC classifications, together with calculated natural atomic charges, in average number of electrons e, of TACs **1** -**9**. Negative charges are coloured in red, and positive charges in blue, and negligible charges in green.

Neither *pseudoradical* nor carbenoid centers appear in TACs **6**, **7**, **8** and **9**, but there are disynaptic basins, V(X1,N2), V'(X1,N2), V(N2,Z3) and V´(N2,Z3), which populations are associated to multiple bonds, thus being considered as zwitterionic TACs.

On the other side, the population of the V(X1,N2) and V(N2,Z3) disynaptic basins associated to the L-TACs indicates that, except to nitrile oxide **7** that has a propargylic structure, X1-N2≡Z3, the other TACs have an allenic structures, X1=N2=Z3.

Finally, 2-methylpropene **10** shows the presence of a pair of disynaptic basins, V(C4,C5) and V(C4,C5), with a total population of 3.52 e, respectively, being associated to a C4−C5 double bonds.
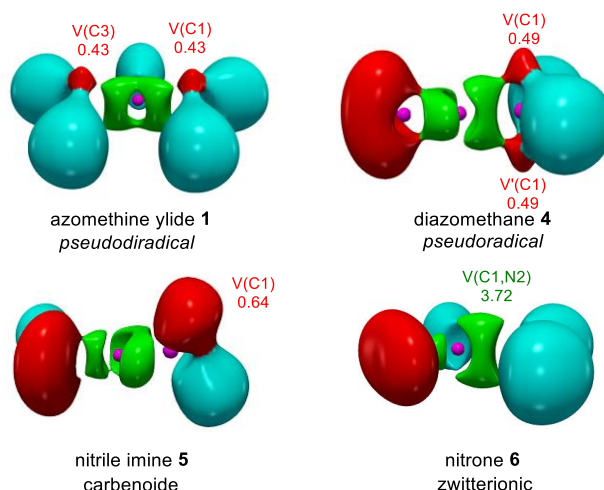

Figure 2. B3LYP/6-311G(d,p) ELF localisation domains represented at an isosurface value of ELF = 0.75, together with the valence basin populations given in average number of electrons, e. of the valence basins charactering the type of TAC of azomethine ylide **1**, *pseudodiradical*, diazomethane **4**, *pseudo(mono)radical*, nitrile imine **5**, carbenoid, and nitrone **6**, zwitterionic. V(C,N) and V(N,N) disynaptic basins are represented in green, V(C,H) disynaptic basin are represented in light blue, V(C) and V(N) monosynaptic basins are represented in red, and C(C) core basins are represented in pink.

ELF topological analysis of the nine TACs **1** – **9** shows that while zwitterionic TACs such as nitrone **6** correspond with the Huisgen's 1,2-dipole structure [43], *pseudodiradical* and *pseudo(mono)radical* TACs, such as azomethine ylide **1** and diazomethane **4**, correspond with the Firestone's radical structures [44]. However, it is interesting to remark that while *pseudodiradical* and *pseudo(mono)radical* TACs are species with a stable closed-shell electronic structure, actual radical species have open-shell electronic structures [42].

NPA analysis of the natural atomic charges at the nine TACs **1** - **9** shows that, except for azide **8** and nitrous oxide **9**, all TACs has the atoms negatively charges (see Figure 2), thus ruling out the commonly accepted charge distribution of a 1,2-zwitterionic

Lewis structure [16]. These atomic change distributions result of the more electronegative character of the C, N and O atoms than that of the H one. Consequently, the anisotropy atomic charge distribution on TACs cannot come from resonant electronic structures, but the anisotropic distribution of the electron density generated by the different atoms belonging to a TAC.[16]

3.2. Analysis of the global and local CDFT reactivity indices, at the GS of the reagents.

The analysis of the reactivity indices based on CDFT has become a useful tool for the study of reactivity in polar reactions [8]. Therefore, in order to establish the polar or non-polar character of these 32CA reactions, an analysis of CDFT reactivity indices was performed. The CDFT indices were calculated at the B3LYP/6-31G(d) computational level since it was used to define the electrophilicity and nucleophilicity scales [8]. The B3LYP/6-31G(d) global indices, namely, the electronic chemical potencial, μ, chemical hardness, η, electrophilicity, ω, and nucleophilicity, N, at the GS of TACs **1** to **9** and 2-methylpropane **10**, are given in Table 3.

Table 3. B3LYP/6-31G(d) global CDFT indices, namely, the electronic chemical potencial, μ, chemical hardness, η, electrophilicity, w, and nucleophilicity, N, in eV, at the GS of TACs **1** to **9** and 2-methylpropane **10**.

Reagent	μ	η	ω	N
1	-1.82	4.47	0.37	5.07
2	-2.83	7.37	0.55	2.61
3	-2.70	5.02	0.72	3.92
4	-3.64	4.73	1.40	3.11
5	-3.43	5.55	1.06	2.92
6	-3.54	5.87	1.07	2.64
7	-3.44	7.87	0.75	1.75
8	-4.24	6.54	1.37	1.62
9	-4.92	8.79	1.37	-0.19
10	-2.83	7.37	0.55	2.60

The electronic chemical potential [7] μ of the nine TACs ranges from -1.81 (**1**) to -4.92 (**9**) eV, while that of 2-methylpropane **10** is -2.83 eV. On the other hand, in general, the hardness [45] η of these TACs increases along this series of TACs. Thus, while azomethyne ylide **1** has a $\eta = 4.47$ eV, azide **9** has a $\eta = 8.79$ eV. Thus, azomethyne ylide **1** is the most softness TAC, while azide **9** is the most hardness TAC.

The electrophilicity ω index [9] of these TACs ranges from 0.37 eV (**1**) to 1.37 (**9**) Thus, while TACS **1**, **2**, **3**, and **7**, are classified as marginal electrophiles, TACs **4**, **5**, **6**, **8** and **9** are classified as moderate electrophiles within the electrophilicity scale [8]. On the other hand, while the nucleophilicity *N* index [10] for TACs **1**, *N* = 5.07 eV, **3**, *N* = 3.92 eV, and **4**, *N* = 3.11 eV, is higher than 3.0 eV, being classified as strong nucleophiles, TACs **2**, *N* = 2.61 eV, **5**, *N* = 2.64 eV, and **6**, *N* = 2.92 eV, are classified as moderate nucleophiles, and TACs **7**, *N* = 1.75 eV, to **9**, *N* = -0.19 eV, having a nucleophilicity *N* index lower than 2.0 eV, are classified as marginal nucleophiles within the nucleophilicity scale [8].

The electrophilicity ω and nucleophilicity *N* indices of 2-methylpropane **10** are 0.55 and 2.60 eV, respectively, being classified as a marginal electrophile and a moderate nucleophile. Thus, while 2-methylpropane **10** will never participate as electrophile in polar reactions, it could participate as nucleophile only towards strong electrophilic species.

As the polar character of organic reactions is mainly controlled by electrophilic species, the low electrophilic character of these species suggests that the corresponding 32CA reactions will have low polar character.

Along a polar reaction involving the participation of non-symmetric reagents, the most favourable reactive channel is that involving the initial two-centre interaction between the most electrophilic centre of the electrophile and the most nucleophilic centre of the nucleophile [6]. In this context, the electrophilic P_k^+ and nucleophilic P_k^- Parr functions [11] derived from the excess of spin electron density reached *via* the GEDT [18] process from the nucleophile toward the electrophile have shown to be the most accurate and insightful tools for the study of the local reactivity in polar and ionic processes. Hence, in order to characterise the regioselectivity in polar 32CA reactions, the P_k^+ electrophilic and P_k^- nucleophilic Parr functions of three selected TACs, a *pseudoradical*, diazomethane **4**, a carbenoid, nitrile imine **5**, and a zwitterionic, nitrone **6** and 2-methylpropane **10**, were analysed (see Figure 3).

Nucleophilic and electrophilic substituted ethylenes have the most nucleophilic and electrophilic centers at the non-substituted CH$_2$ carbon of the ethylene [24]; see the P_k^+ electrophilic and P_k^- nucleophilic Parr functions of 2-methylpropane **10** in Figure 3.

Analysis of the nucleophilic P_k^- and electrophilic P_k^+ Parr functions of the three selected TACs shows that along polar 32CA reactions, a change in regioselectivity will be expected depending on if the reaction is classified of FEDF or REDF [20]. As many of the TACs are strong nucleophiles, see Table 3, analysis of the electrophilic P_k^+ Parr functions will permit to predict the regioselectivity in a FEDF 32CA reaction.

Interestingly, zwitterionic nitrone **6** shows a reverse regioselectivity than *pseudoradical* diazomethane **4** and carbenoid nitrile imine **5**. Thus, while diazomethane **4** and nitrile imine **5** present the most nucleophilic center at the *pseudoradical* and carbenoid C1 carbons, nitrone **6** presents the most nucleophilic centre at the O3 oxygen.
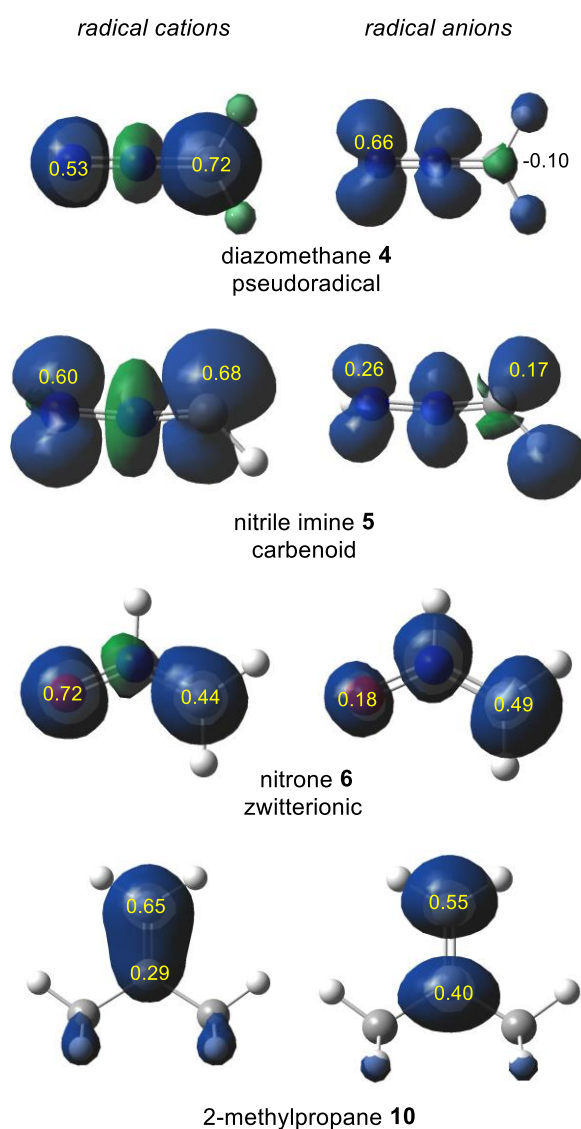

Figure 3. 3D representations of the Mulliken atomic spin densities of the radical cation and radical anion of, diazomethane **4**, nitrile imine **5**, nitrone **6**, and 2-methylpropane **10,** together with the nucleophilic P_k^- and electrophilic P_k^+ Parr functions.

*3.3 Study of the reactivity and regioselectivity in the 32CA reactions of TACs **1** - **9** with 2-methylpropene **10***

Except for azomethine ylide **1**, all reagents do not present molecular symmetry; hence eight of the selected 32CA reactions can occur through two competitive regioisomeric reaction paths; the first ones, denoted as *r1*, are related to the initial formation of the X1–C4 single bond, while the second one, denoted as *r2*, are associated to the formation of the Z3–C4 one (see Scheme 5). Searching of the stationary points along each of the two regioisomeric reaction paths revealed only one TS and its corresponding cycloadduct; thus these 32CA reactions are meant to occur through one-step mechanism. Relative energies of the stationary points involved in the nine 32CA reactions are given in Table 4.
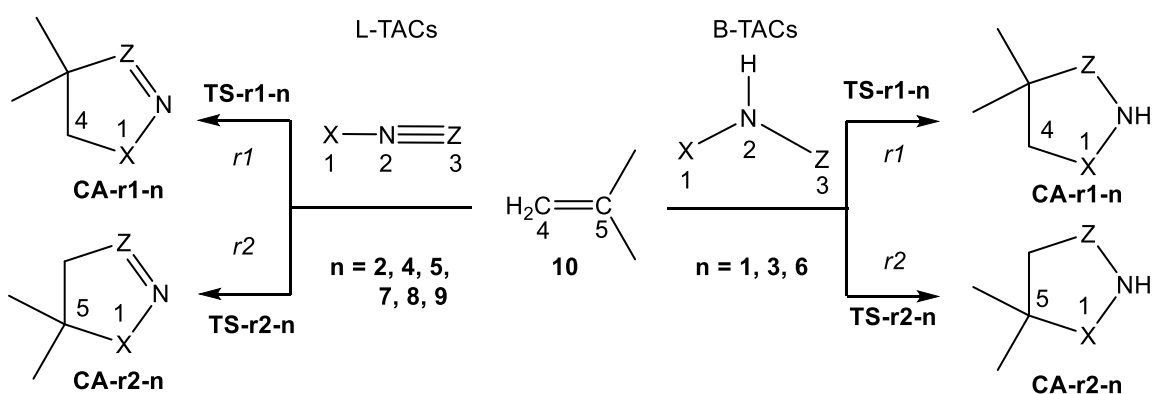
Scheme 5. Regioisomeric reaction paths associated to the 32CA reactions of TACs **1** - **9** with 2-methylpropene **10**.

The activation energies associated to the nine 32CA reactions range from 8.8 (**1**) to 27.7 (**9**) kcal·mol^{-1}, the reactions being exothermic between 2.9 (**9**) and 59.5 (**2**) kcal·mol^{-1}. Some appealing conclusions can be drawn from the relative energies given in Table 4: i) the most favourable 32CA reaction corresponds to that involving *pseudodiradical* azomethyne ylide **1**, $\Delta E_{act} = 8.8$ kcal·mol^{-1}, while the most unfavourable one corresponds to that involving zwitterionic nitrous oxide **9**, $\Delta E_{act} = 27.7$ kcal·mol^{-1}; ii) except for diazomethane **4**, the general trend of reactivity *pdr-type > pmd-type > cb-type > zw-type* is observed [16]; iii) except for the 32CA reaction involving azide **8**, which is low *r2* regioselective [25], seven of these 32CA reactions are *r1* regioselective. Note that in the case of nitrone **6**, the *r1* regioselectivity is opposite to that observed in polar *zw-type*

32CA reactions involving electrophilic ethylenes [24]; iv) the regioselectivity, measured as $\Delta\Delta E_{act}$, ranges from 1.0 kcal·mol^{-1} for the 32CA reaction involving nitrile ylide **2** to 5.3 kcal·mol^{-1} for the 32CA reaction involving nitrone **6**; excluding TACs **1**, **2** and **8**, the other four 32CA reactions can be considered highly *r1* regioselective to be $\Delta\Delta E_{act} > 2.5$ kcal·mol^{-1}; v) considering the strong exothermic character of the 32CA reactions of TACs **1** – **7**, $\Delta E_{reac} > 22.3$ kcal·mol^{-1}, these reactions can be considered as irreversible, and consequently, formation of the *r1* regioisomeric cycloadducts is kinetically controlled; and vi) in general, except for diazomethane **4**, all *r1* regioisomeric cycloadducts are thermodynamically more stable than the *r2* ones. Consequently, except for TACs **4** and **8**, these 32CA reactions can also be considered thermodynamically controlled *r1* regioselective.

Considering that in the series of TACs **2** – **9** the ends X1 atom is lesser electronegative than the Z3 one, *i.e.* the electronegativity increases in the order C < N < O, and trigonal planar (sp^2) < linear (sp), it is possible to conclude that the *r1* regioselectivity observed in these 32CA reactions is kinetically controlled by the interactions between the least electronegative ends X1 atom of these TACs and the methylene C4 carbon of 2-methylpropane **10**.

Table 5. Relative electronic energies, ΔE, in kcal·mol^{-1}, of TSs and cycloadducts involved in the 32CA reactions of TACs **1** to **9** with 2-methylpropene **10**.

TAC	*type*	**TS-r1-n**	**TS-r2-n**	**CA-r1-n**	**CA-r1-n**
1	*pdr*	8.8		-54.6	
2	*cb*	14.0	15.0	-59.5	-59.4
3	*pmr*	12.8	15.3	-39.7	-36.7
4	*pmr*	20.4	23.1	-23.1	-27.0
5	*cb*	11.8	14.4	-54.0	-51.3
6	*zw*	14.4	19.8	-27.1	-22.0
7	*zw*	15.0	19.9	-38.3	-32.7
8	*zw*	23.7	23.1	-17.3	-16.7
9	*zw*	27.7	30.5	-2.9	-1.3

The optimized geometries of the most favourable *r1* regioisomeric TSs are shown in Figure 4, while the distances between C–C, C–N and C–O interacting centers at the two regioisomeric TSs are given in Table 6. Some appealing conclusions can be drawn from these geometrical parameters: i) the distance between the interacting centres at the

r1 regioisomeric TSs ranges from 2.442 (C–C) Å at **TS-r1-1** to 1.995 (C–N) at **TS-r1-9**; ii) the C–X (C,N,O) distances decrease with the increase of the activation energy; i.e. the more unfavourable the TS, more advanced is; iii) considering that the formation of the C–C, C–N and C–O single bonds begins in the short ranges of 2.00 - 1.99, 1.90 - 1.80 and 1.80 - 1.70 Å [16], respectively, these distances indicate that the formation of the C–X (C,N,O) new single bonds do not have started at any TS (see Section 3.4); and, finally iv) except for **TS-r1-2**, the distance involving the ends X1 atom of these TACs is shorter that that involving Z3 one. These behaviours point out that the interaction between the least electronegative X1 atom of these TACs with the methylene C4 carbon of **10** is lesser unfavourable and more advanced that that involving the more electronegative Z3 atom.
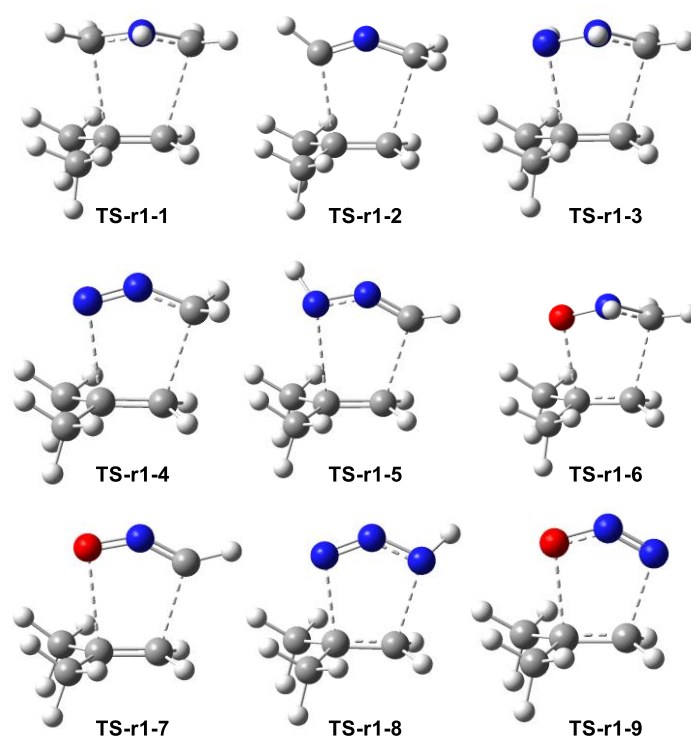

Figure 4. Geometries of the most favorable *r1* regioisomeric TSs involved in the 32CA reactions of TACs **1** to **9** with 2-methylpropene **10**.

Table 6. Cx-Xy (X = C, N, O) distances, in angstroms Å, at the *r1* and *r2* regioisomeric
TSs involved in the 32CA reactions of TACs **1** to **9** with 2-methylpropene **10**.

TAC	**TS-r1-n**		**TS-r2-n**	
n	C4-X1	C5-X3	C4-X3	C5-X1
1	2.442	2.445		
2	2.423	2.415	2.471	2.374
3	2.266	2.319	2.308	2.239
4	2.234	2.324	2.280	2.228
5	2.222	2.534	2.392	2.276
6	2.174	2.213	2.140	2.160
7	2.192	2.483	2.352	2.182
8	2.131	2.140	2.054	2.189
9	1.995	2.176	2.083	2.028

In order to evaluate the polar nature of these 32CA reactions, the GEDT [18] at the
TSs was analysed. Reactions with GEDT values below 0.05 e correspond to non-polar
processes, while values above 0.2 e correspond to polar processes. The GEDT values
measured at the TAC framework of the more favourable *r1* regioisomeric TSs are 0.14 e
at **TS-r1-1**, −0.09 e at **TS-r1-2**, 0.07 e at **TS-r1-3**, 0.07 e at **TS-r1-4**, −0.03 e at **TS-r1-5**,
−0.01 e at **TS-r1-6**, −0.05 e at **TS-r1-**7, −0.08 e **TS-r1-8** and −0.19 e at **TS-r1-9**. Some
appealing conclusions can be drawn from these GEDT values: i) while the 32CA reactions
of azomethine ylide **1** and nitrous oxide **9** have polar character, those of TACs **2** – **8** have
a low or non-polar character; ii) while the 32CA reaction of azomethine ylide **1** is
classified as the FEDF, that of nitrous oxide **9** is classified as the REDF[20]. Note the
change of the sing of the GEDT at **TS-r1-1**, 0.14 e, and at **TS-r1-9**, −0.19 e; thus, while
azomethine ylide **1** acts as electron-donor, nitrous oxide **9** acts as electron-acceptor. This
is a consequence of the strong nucleophilic character of **1** and the strong electrophilic
character of **9** (see Table 3); and finally, iii) the non-polar 32CA reactions of nitrile imine
5 and nitrone **6** can be classified as the NEDT.

3.4. ELF topological analysis of the most favourable r1 regioisomeric TSs.

Finally, the electronic structure of the more favourable *r1* regioisomeric TSs was analysed
through a topological analysis of the ELF. The ELF basin populations of the nine TSs are

given in Table 7, while a picture of the ELF basin attractor positions of the TSs is shown in Figure 5.

Analysis of the basin populations of the nine TSs shows that they present great similitudes. All TSs show a V(N2) monosynaptic basin, with a population ranking from 0.73 e (**TS-r1-1**) to 2.33 e (**TS-r1-9**). In general, the population of these V(N2) monosynaptic basins increase with the advanced character of the TS. Thus, the population of this monosynaptic basin, which comes mainly of the depopulation of the X1−N2 bonding region of the TACs, reaches the maximum value at the final cycloadducts. These V(N2) monosynaptic basins, which are not present at the TACs (see Table 2), are associated to the N2 non-bonding electron density presents at the final cycloadduct.

All ends C1 and C3 carbons present one or two V(C) monosynaptic basins, integrating between 0.51 e (**TS-r1-1**) to 1.47 e (**TS-r1-6**). Interestingly, while these V(C) monosynaptic basins are already present at the *pseudoradical* and carbenoid TACs, they must be created at the zwitterionic TACs such as nitrone **6** and nitrile oxide **7** by depopulation of the C1−N2 bonding region. This behaviour, together with the creation of the V(N2) monosynaptic basin, account for the high activation energies of the TSs associated to the *zw-type* 32CA reactions [16]. Note that these V(Ci) monosynaptic basins are demanded for the subsequent C−C single bond formation [18].

Except for the unfavourable **TS-r1-9**, the N and O centers show the presence of a V(N) or V(O) monosynaptic basin, associated to a N or O non-bonding electron density, which are already present at the corresponding TACs. Note that the formation of the subsequent N−C or O−C singe bonds result of the participation of the part of the non-bonding electron density of the N or O atoms and that of the *pseudoradical* carbon of the ethylene.

Finally, ELF of the ethylene framework shows the presence of one V(C4,C5) disynaptic basin, integrating between 3.06 e (**TS-r1-9**) and 3.41e ((**TS-r1-1**). Along the reaction path, ongoing from the separated reagents to TSs, the C−C bonding region of 2-methylpropene **10** is depopulated in order to generate, after to pass the TSs, the V(C4) and V(C5) monosynaptic basins required for the formation of the new X−C single bonds. As a consequence of this continue depopulation, the two V(C4,C5) and V'(C4,C5) disynaptic basins present at 2-methylpropene **10**, have merged into one V(C4,C5) disynaptic basin at the nine TSs.

From the ELF topological analysis of the nine TSs, one relevant conclusion can be drawn. Considering the unlike behaviour of the ends C, N and O centers, the nine TSs present a similar electronic structure; all ends carbons of the TACs have one V(C1) monosynaptic basin associated to a *pseudoradical* or carbene center, while the ends nitrogen and oxygen centers have V(N) or V(O) monosynaptic basins associated to N or O non-bonding electron density regions. Only changes in the population of these V(X) monosynaptic basins with the advanced character of the TSs are found. On the other hand, the C4–C5 double bonding region of the ethylene framework shows also a depopulation, which increase also with the advanced character of the TS. However, neither V(C4) nor V(C5) monosynaptic basin are observed in the ethylene framework at the nine TSs.

As the activation energies associated to these non-polar 32CA reactions are mainly associated to the depopulation of the N2–X1 and C4–C5 bonding regions, which is required for the formation of the non-bonding electron density regions, i.e. the *pseudoradical* centers in carbon atoms [23,24], at the interacting centers, the dissimilar activation energies found in these 32CA reactions depend on the presence of the V(X1) (X = C,N,O) monosynaptic basins at the corresponding TACs, thus justifying the order of reactivity *pseudodiradical > pseudoradical* > carbenoid > zwitterionic.

Table 7. ELF basin populations of the TSs associated to *r1* regioisomeric reaction path of the 32CA reactions of TACs **1** to **9** with 2-methyl propene **10**, in average number of electrons (e).

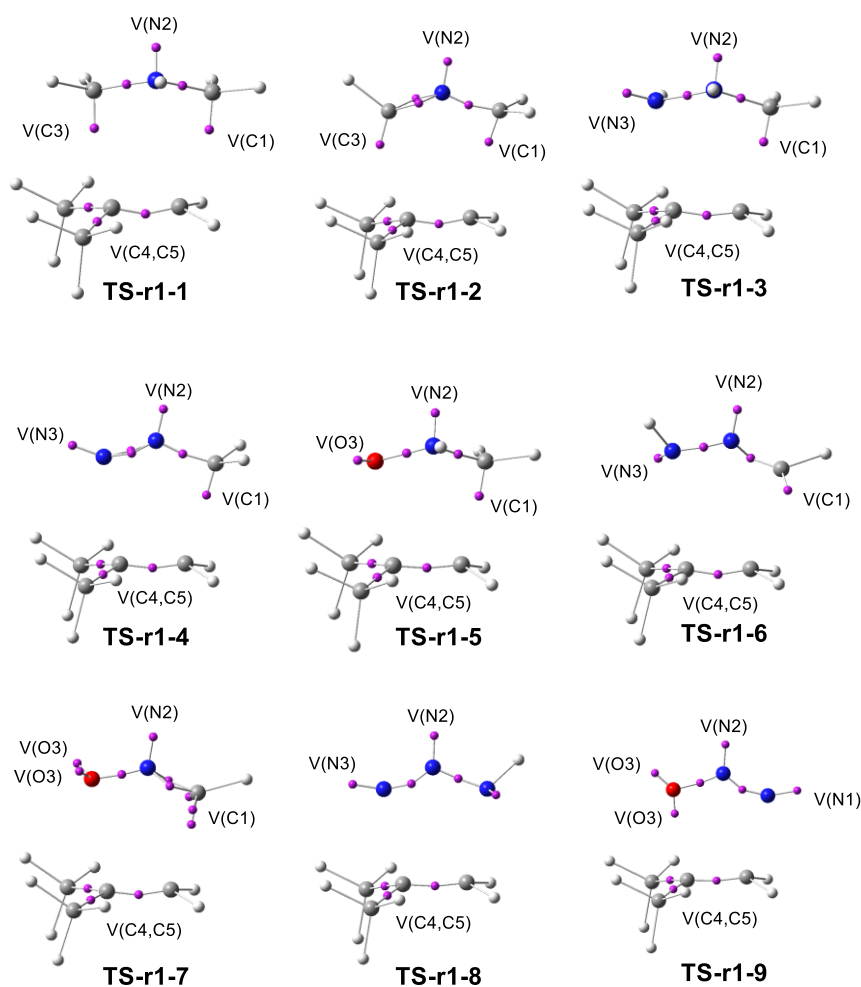|	TS-r1-1	TS-r1-2	TS-r1-3	TS-r1-4	TS-r1-5	TS-r1-6	TS-r1-7	TS-r1-8	TS-r1-9
V(X1)	0.63	0.51	0.59	0.91	0.44	1.47	1.33	3.38	3.84
V(X1,N2)	2.32	2.24	2.31	1.92	2.39	2.93	1.55	2.71	2.72
V'(X1,N2)							1.55		
V(N2)	0.73	1.54	1.12	1.97	1.32	2.09	2.04	2.26	2.33
V(N2,Z3)	2.30	1.67	1.71	1.55	1.24	1.88	1.49	2.71	1.44
V'(N2,Z3)		1.67		1.43					
V(Z3)	0.73	1.63	3.35	3.75	2.86	3.32	2.82	3.87	5.22
V´(Z3)					2.99		2.82		0.40
V(C4,C5)	3.41	3.30	3.35	3.31	3.25	3.23	3.20	3.14	3.06

Figure 5. ELF basin attractor positions of the TSs associated to *r1* regioisomeric reaction path of the 32CA reactions of TACs **1** to **9** with 2-methyl propene **10**.

Finally, the V(C1) monosynaptic basins present at the TSs, which are associated with a *pseudoradical* or carbenoid center required for the subsequent C1−C4 single bond formation, appear at the least electronegative ends carbon atom of these TAC. As in zwitterionic TACs, these V(C1) monosynaptic basins are created by the depopulation of the neighboring C1−N2 bonding region, they demand a higher energy cost. On the other hand, in TACs in which the formation of the X1−C4 single bond involves the participation of a nitrogen or oxygen atom, formation of these X1−C4 single bonds demands the donation of part of the non-bonding electron density of these heteroatoms. Consequently, it is reasonable to understand that the changes in electron density required for the formation of the new X1−C4 single bonds will take place more easily at the ends center

involving the least electronegative X1 atom. These behaviors account for the regioselectivity found in these non-polar 32CA reactions.

5. Conclusions

The 32CA reactions of nine simplest TACs **1** - **9** with 2-methylpropene **10** have been studied within MEDT at the MPWB1K/6-311G(d,p) computational level in order to understand the origin of the regioselectivity in non-polar 32CA reactions.

Topological analysis of the nine simplest TACs **1** - **9** allows their classification into one of the four types of TACs: *pseudodiradical*, *pseudo(mono)radical*, carbenoid, zwitterionic ones. On the other hand, the NPA shows that many of the atoms of these TACs are negatively charged, thus ruling out the commonly accepted charge distribution of a 1,2-zwitterionic Lewis structure.

The CDFT classifies TACs **1**, **2**, **3** and **7** as marginal electrophiles, and TACs **4**, **5**, **6**, **8** and **9** as moderate electrophiles. On the order hand, TACs **1**, **3** and **4** are classified as strong nucleophiles, TACs **2**, **5** and **6** as moderate nucleophiles, and TACs **7** to **9** as marginal nucleophiles. Consequently, only TACs **1**, **3**, and **4** will participate in polar 32CA reactions as strong nucleophiles.

The activation energies associated to the nine 32CA reactions range from 8.8 (**1**) to 27.7 (**9**) kcal·mol^{-1}, the reactions being exothermic between 2.9 (**9**) and 59.5 (**2**) kcal·mol^{-1}. The general trend of reactivity, *pdr-type > pmd-type > cb-type > zw-type*, is observed in this series of 32CA reactions. Except for the 32CA reaction involving azide **8**, which is low *r2* regioselective, all these 32CA reactions are *r1* regioselective.

Analysis of the geometries of the more favourable *r1* regioisomeric TSs indicates that the distance between the interacting centres ranges from 2.442 (C–C) Å at **TS-r1-1** to 1.995 (C–N) at **TS-r1-9**. The C–X (X = C,N,O) distances decrease with the increase of the activation energy; i.e. the more unfavourable the TS, more advanced is. Except for **TS-r1-2**, the distance involving the ends X1 atom of these TACs is shorter that that involving ends Z3 atom. These behaviours point out that in these non-polar 32CA reactions, the interactions between the least electronegative X1 atom of these TACs and the methylene C4 carbon of **10** are lesser unfavourable and more advanced that that involving the most electronegative Z3 atom.

The computed GEDT values at the more favourable *r1* regioisomeric TSs indicate that while the 32CA reactions of TACs **1** and **9** have polar character, those of TACs **2** – **8** have a low polar or non-polar character.

A comparative analysis of the ELF of the more favourable *r1* regioisomeric TSs shows that they a present a similar electronic structure. As the activation energies associated to non-polar cycloaddition reactions are mainly associated to the depopulation of the N2–X1 and C4–C5 bonding regions demanded for the formation of the new V(X) monosynaptic basins, the different activation energies observed in these 32CA reaction depend on the presence of V(C) monosynaptic basins at the TACs, thus justifying the order of reactivity *pseudodiradical > pseudoradical >* carbenoid > zwitterionic.

From this MEDT study it is possible to conclude that the lesser energetic cost demanded for the creation of the non-bonding electron density at the least electronegative X1 atom, which is required for the subsequent X1–C4 single bond formation, is responsible for the regioselectivity of these low polar 32CA reactions.

Author Contributions: L.R.D. headed the subject, wrote the manuscript and performed calculations; M.R.G headed the subject, performed calculations and wrote the manuscript; and J.C.S. performed calculations and wrote the manuscript.

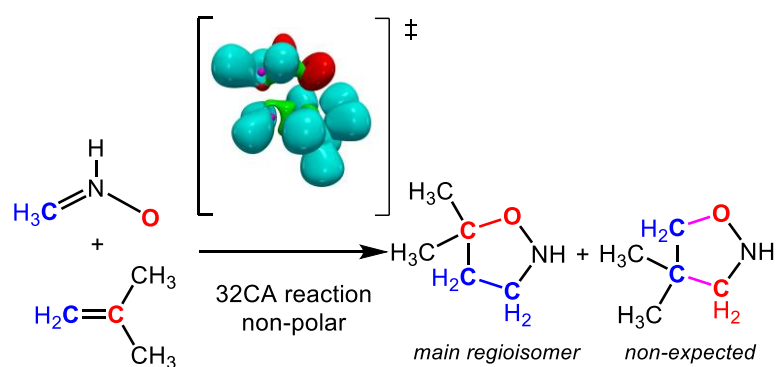**Conflicts of interest:** There are no conflicts to declare.

References

(1)   Moss, G. P.; Smith, P. A. S.; Tavernier, D. Pure Appl. Chem. 1995, 67, 1307.

(2)   Carruthers, W. Some Modern Methods of Organic Synthesis; second ed.; Cambridge University Press: Cambridge, 1978.

(3)   Carruthers, W. Cycloaddition Reactions in Organic Synthesis; Pergamon: Oxford,1990.

(4)   Padwa, A. 1,3-Dipolar Cycloaddition Chemistry; Wiley-Interscience: New York, 1984; Vol. 1-2.

(5)   Domingo, L.R.; Aurell, M.J.; Perez, P.; Contreras, R. Quantitative characterization of the local electrophilicity of organic molecules. Understanding the regioselectivity on Diels-Alder reactions. *J. Phys. Chem. A*, **2002**, *106*, 6871-6875.

(6)   Aurell, M.J.; Domingo, L.R.; Pérez, P., Contreras, R. A theoretical study on the regioselectivity of 1,3-dipolar cycloadditions using DFT-based reactivity indexes. *Tetrahedron* **2004** , *60*, 11503–11509

(7)   Parr, R.G.; Yang, W. Density functional theory of atoms and molecules, Oxford University Press, New York, 1989.

(8)   Domingo, L.R.; Ríos-Gutiérrez, M.; Pérez, P. Applications of the conceptual density functional indices to organic chemistry reactivity. *Molecules* **2016**, *21*, 748.

(9)   Parr, R.G. Szentpaly, L.v.; Liu, S. Electrophilicity index. *J. Am. Chem. Soc.*, **1999**, *121*, 1922-1924.

(10)   Domingo, L.R.; Chamorro, E.; Pérez, P. Understanding the reactivity of captodative ethylenes in polar cycloaddition reactions. A theoretical study. *J. Org. Chem.*, **2008**, *73*, 4615-4624.

(11)   Domingo, L.R.; Pérez, P; Sáez, J.A. Understanding the local reactivity in polar organic reactions through electrophilic and nucleophilic Parr functions. *RSC Adv*. **2013**, *3*, 1486-1494.

(12)   Domingo, L.R. Molecular electron density theory: a modern view of reactivity in organic chemistry. *Molecules* **2016**, *21*, 1319.

(13)   Fukui, K. *Molecular Orbitals in Chemistry, Physics, and Biology,* New York, 1964.

(14)   Becke, A.D. Edgecombe, K.E. A simple measure of electron localization in atomic and molecular-systems. *J. Chem. Phys.* **1990**, *92*, 5397-5403.

(15)   Bader, R.F.W. Atoms in Molecules: A Quantum Theory: Clarendon Press, USA, 1994.

(16)   Ríos-Gutiérrez, M.; Domingo, L.R. Unravelling the mysteries of the [3+2] cycloaddition reactions. *Eur. J. Org. Chem.* **2019**, 267–282.

(17)   Domingo, L.R.; Sáez J.A., Understanding the mechanism of polar Diels–Alder reactions. *Org. Biomol. Chem.* **2009**, *7*, 3576-358.

(18)   Domingo, L.R. A new C-C bond formation model based on the quantum chemical topology of electron density. *RSC Adv.* **2014**, *4*, 32415–32428.

(19) Domingo, L.R; Ríos-Gutiérrez, M.; Pérez. P. How does the global electron density transfer diminish activation energies in polar cycloaddition reactions? A Molecular Electron Density Theory study. *Tetrahedron 2017*, *73*, 1718-1724.

(20) Domingo, L.R.; Ríos-Gutiérrez, M.; Pérez, P. A Molecular Electron Density Theory Study of the Reactivity of Tetrazines in Aza-Diels-Alder Reactions. *RSC Adv.* **2020**, *10*, 15394–15405.

(21) Houk, K. N.; González, J.; Li, Y. Pericyclic reaction transition states: passions and punctilios, 1935-1995. *Acc. Chem. Res.* **1995**, *28*, 81-90.

(22) Sustmann, R.; Trill, H. Substituent Effects in 1,3-Dipolar Cycloadditions of Phenyl Azid *Angew. Chem. Int. Ed. Engl.* 1972, **11**, 838–840.

(23) Domingo, L.R.; Mar Ríos-Gutiérrez, M.; Silvi, B.; Pérez; P. The Mysticism of Pericyclic Reactions: A Contemporary Rationalisation of Organic Reactivity Based on Electron Density Analysis. *Eur. J. Org. Chem.* **2018**, 1107–1120.

(24) Domingo, L.R.; Ríos-Gutiérrez, M.; Pérez, P. A Molecular electron density theory study of the reactivity and selectivities in [3 + 2] cycloaddition reactions of C,N-dialkyl nitrones with ethylene derivatives. *J. Org. Chem.* **2018**, *83*, 2182–2197.

(25) El Ayouchia, H. B.; Lahoucine, B.; Anane, H.; Ríos-Gutiérrez, M.; Domingo, L.R.; Stiriba, S.-E. Experimental and Theoretical MEDT Study of the Thermal [3+2] Cycloaddition Reactions of Aryl Azides with Alkyne Derivatives. *ChemistrySelect* **2018**, *3*, 1215–1223.

(26) Becke, A.D. Density-functional thermochemistry. The role of exact Exchange. *J. Chem. Phys.* **1993**, *98*, 5648–5652.

(27) Lee, C.; Yang, W.; Parr, R.G. Development of the Colle-Salvetti correlation-energy formula into a functional of the electron density. *Phys. Rev. B* **1988**, *37*, 785–789.

(28) Hehre, M.J.; Radom, L.; Schleyer, P.v.R.; Pople, J. Ab initio Molecular Orbital Theory, Wiley, New York, 1986.

(29) Schlegel, H.B. Optimization of equilibrium geometries and transition structures. *J. Comput. Chem.* **1982**, *3*, 214-218.

(30) Schlegel, H.B. In modern electronic structure theory, Yarkony, D.R., Ed., World Scientific Publishing, Singapore, **1994**.

(31) Fukui, K. Formulation of the reaction coordinate. *J. Phys. Chem.* **1970**, *74*, 4161–4163.

(32) González, C.; Schlegel, H. B. Reaction path following in mass-weighted internal coordinates. *J. Phys. Chem.* **1990**, *94*, 5523–5527.

(33)   González, C.; Schlegel, H. B. Improved algorithms for reaction path following: higher-order implicit algorithms. *J. Chem. Phys.* **1991**, *95*, 5853–5860.

(34)   Reed, A.E.; Weinstock, R.B.; Weinhold, F. Natural population analysis. *J. Chem. Phys.*, **1985**, *83*, 735-746.

(35)   Reed, A.E.; Curtiss, L.A.; Weinhold, F. Intermolecular interactions from a natural bond orbital, donor-acceptor viewpoint. *Chem. Rev.*, **1988**, *88*, 899-926.

(36)   Gaussian 16, Revision A.03, Frisch, M.J.; Trucks, G.W.; Schlegel, H.B.; Scuseria, G.E.; Robb, M.A.; Cheeseman, J.R.; Scalmani, G.; Barone, V.; Petersson, G. A.; Nakatsuji, H.; et al. Gaussian, Inc., Wallingford CT, **2016**.

(37)   Noury, S.; Krokidis, X.; Fuster, F.; Silvi, B. Computational tools for the electron localization function topological analysis. *Comput. Chem.* **1999**, *23*, 597-604.

(38)   GaussView, Version 6.0, Dennington, R.; Keith, T.A.; Millam, J.M., Semichem Inc., Shawnee Mission, KS, **2016**.

(39)   Ahrens, J.; Geveci, B.; Law, C. ParaView: An End-User Tool for Large Data Visualization, Visualization Handbook, Elsevier, 2005, ISBN-13:978 - 0123875822.

(40)   Ayachit, U. The ParaView Guide: A Parallel Visualization Application, Kitware, 2015, ISBN 978-1930934306.

(41)   Silvi, B.; Savin, A. Classification of chemical bonds based on topological analysis of electron localization functions. *Nature*, 1994, *371*, 683-686.

(42)   Domingo, L.R.; Sáez, J.A., Understanding the Electronic Reorganization along the Nonpolar [3 + 2] Cycloaddition Reactions of Carbonyl Ylides *J. Org. Chem.* **2011**, 76, 373-379.

(43)   Huisgen, R. 1,3-Dipolar cycloadditions. 76. Concerted nature of 1,3-dipolar cycloadditions and the question of diradical intermediates. *J. Org. Chem.* **1976**, *41*, 403-419.

(44)   Firestone, R.A. Mechanism of 1,3-dipolar cycloadditions. *J. Org. Chem.* **1968**, *33*, 2285-2290.

(45)   Parr, R.G.; Pearson, R.G. Absolute hardness: Companion parameter to absolute electronegativity. J. Am. Chem. Soc. 1983, 105, 7512–7516.

Graphical Abstract

Regioselectivity in non-polar [3+2] cycloaddition reactions